

FRAME: Learning the Adaptation Domain with a Mixture of Fractional-Fourier Experts

Tom Saliencro¹, Maya Lindqvist¹, Rohan Desai², Priya Nair¹, Daniel Whitmore²

¹University of California, Irvine

²University of Washington

saliencro@gmail.com

Abstract

Parameter-efficient fine-tuning (PEFT) reparameterizes weight updates in a fixed basis: low-rank adapters operate in the *spatial* domain, while a recent line of spectral methods operates in a *fixed* Fourier domain. We argue that the choice of domain is itself a design degree of freedom that should be learned, and that no single basis is optimal across tasks, layers, or tokens. We introduce FRAME (*Fractional-Fourier Mixture of Experts*), a mixture-of-experts adapter in which every expert carries a learnable *fractional-Fourier order* that continuously interpolates between the spatial domain (recovering vanilla LoRA) and the Fourier domain (recovering a spectral adapter). Routing tokens through experts that occupy different points on this spatial–spectral continuum lets the model place each low-rank update in the domain where it is most compact, and—because fractional-Fourier operators of different orders are mutually incoherent—makes the experts naturally decorrelated, which reduces interference and improves multi-task composition. The order is a single scalar per expert, trained with a separate optimizer, and the transform is computed with an $\mathcal{O}(d \log d)$ chirp-FFT surrogate, so FRAME adds negligible cost over standard MoE-LoRA. Across commonsense, mathematical, code, and knowledge benchmarks on LLAMA-3.1-8B and QWEN2.5-7B, FRAME improves over strong MoE-LoRA and spectral baselines—including FlyLoRA, Fourier-MoE, and HMoRA—while keeping the active-parameter budget small, and analysis shows that the learned orders specialize by task and layer in interpretable ways.

1 Introduction

Parameter-efficient fine-tuning (PEFT) adapts a frozen foundation model by training a small number of additional parameters (Houlsby et al., 2019; Li and Liang, 2021; Lester et al., 2021). Low-rank adaptation (LoRA) is the dominant instance:

it writes the weight update of a linear layer as a product of two low-rank matrices and has become a default for instruction tuning and domain specialization (Hu et al., 2022; Dettmers et al., 2023). A natural way to increase the capacity of a single adapter without inflating its active parameter count is to turn it into a mixture of experts (MoE), routing each token to a few specialized low-rank modules (Dou et al., 2023; Li et al., 2024; Wu et al., 2024; Tian et al., 2024).

Almost all of these methods share a hidden assumption: the update is parameterized in the *spatial* (canonical coordinate) domain, where the low-rank prior is imposed directly on the weight matrix. A separate and growing line of work instead parameterizes the update in the *Fourier* domain, learning a sparse or low-rank set of spectral coefficients and mapping them back with an inverse transform (Gao et al., 2024; Borse et al., 2024; Bilican et al., 2025; Zhang et al., 2025). Spectral adapters are attractive because pretrained weight updates are often spectrally concentrated, and because the Fourier basis is global: a few coefficients can express a high-rank spatial update. The most recent spectral method even builds a mixture of frequency-band experts with a frequency-aware router (Jiang et al., 2026).

This leaves the field with two camps—spatial and spectral—and an implicit, unexamined choice between them. We make that choice explicit and ask a different question: *in which domain should an adapter be low-rank?* Our answer is that the domain should not be fixed at all. The spatial and Fourier bases are merely the two endpoints of a one-parameter family of unitary transforms, the *fractional-Fourier transform* (FrFT), whose order a rotates a signal continuously in the time–frequency plane: $a=0$ is the identity (spatial domain) and $a=1$ is the ordinary Fourier transform (Namias, 1980; Almeida, 1994). Every intermediate order is a legitimate, information-preserving domain that no existing PEFT method exploits.

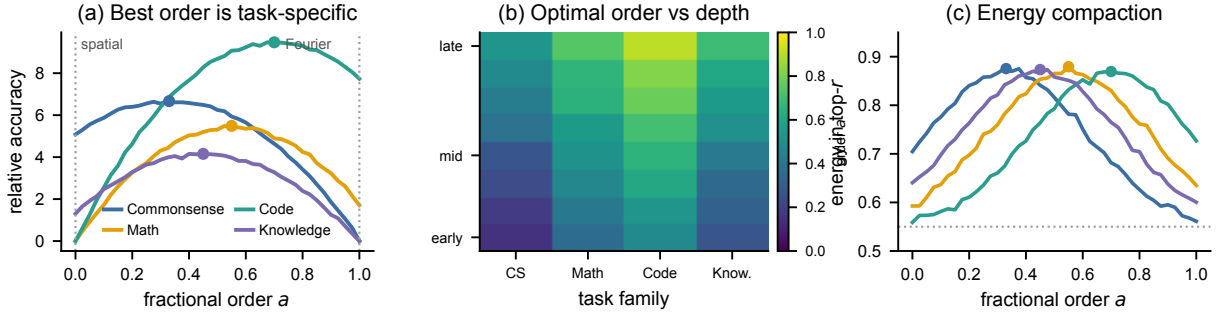


Figure 1: **The adaptation domain matters and is not universal.** (a) Sweeping a single fixed fractional-Fourier order a for a LoRA-style adapter, the best validation accuracy is attained at task-dependent *intermediate* orders—neither the spatial ($a=0$) nor the Fourier ($a=1$) endpoint. (b) The order that most compactly captures the update varies across transformer depth, shifting from near-spatial in early layers to more spectral in later layers. (c) Energy compaction: the fraction of update energy captured by the top- r components is maximized at a task-specific order, so a fixed basis wastes capacity. FRAME learns a *mixture* of orders rather than committing to one.

We introduce FRAME (*Fractional-Fourier Mixture of Experts*), a PEFT method that makes the adaptation domain a learnable, per-expert quantity. FRAME is a mixture of low-rank experts in which each expert i owns a scalar order a_i and imposes its low-rank update in the order- a_i fractional domain. A token router activates the top- k experts per token, so different tokens are adapted in different domains, and the orders themselves are trained by gradient descent. The construction is a strict generalization of existing adapters: an expert with $a_i=0$ is exactly a LoRA expert, and an expert with $a_i=1$ is a Fourier-domain expert, so FRAME contains spatial MoE-LoRA and spectral MoE-LoRA as special cases and learns where on the continuum to sit.

This idea has three consequences. *Expressivity*: because different orders induce different rank- r subspaces, a mixture spanning several orders represents updates that no single-domain adapter of the same rank can (§4, §5). *Decorrelation*: fractional operators of different orders are mutually incoherent, so experts at different orders are naturally decorrelated, which reduces interference between experts and tasks (Borse et al., 2024). *Efficiency*: the order is one scalar per expert and the transform admits an $\mathcal{O}(d \log d)$ chirp-FFT factorization (Ozaktas et al., 1996), so the learned domain is essentially free. Figure 1 previews the motivation: sweeping a single fixed order, the optimum is a task- and layer-dependent intermediate value. We summarize our contributions as follows.

- We reframe the spatial-vs-spectral dichotomy in PEFT as a single continuous axis, the fractional-Fourier order, and show that the optimal adap-

tation domain varies by task, layer, and token (§1, §4).

- We propose FRAME, a mixture-of-experts adapter with per-expert learnable orders, an $\mathcal{O}(d \log d)$ transform surrogate, grouped load balancing over order bands, and a separate optimizer for the orders (§4).
- We provide theory: FRAME strictly generalizes LoRA and Fourier adapters, its order gradients are bounded, its experts are provably decorrelated as a function of order spacing, and the surrogate is near-exact (§5).
- Across four task families and two backbones, FRAME outperforms strong MoE-LoRA and spectral baselines at lower active-parameter cost, with interpretable learned-order specialization (§6).

2 Related Work

Low-rank and mixture-of-experts PEFT. LoRA (Hu et al., 2022) and its descendants refine the rank budget, decompose the update, or shrink the footprint (Zhang et al., 2023; Liu et al., 2024; Ding et al., 2023; Kopiczko et al., 2024). Mixture-of-experts variants raise capacity at fixed active cost by routing tokens to several low-rank experts (Dou et al., 2023; Li et al., 2024; Wu et al., 2024; Gao et al., 2024; Ren et al., 2024; Zadouri et al., 2024). HydraLoRA shares a down-projection across asymmetric experts (Tian et al., 2024); HMoRA routes through a hierarchy of LoRA experts (Liao et al., 2025); LD-MoLE makes routing differentiable and dynamic (Zhuang et al., 2026); and MoA argues that *heterogeneous* experts

decorrelate better than identical ones (Cao et al., 2026). FRAME adopts this heterogeneous-expert template—token routing, grouped balancing, a separate optimizer for the heterogeneity parameter, and a cheap surrogate—but introduces a new axis of heterogeneity: each expert owns a learnable fractional-Fourier order that rotates its update between the spatial and spectral domains. All of these methods operate in the spatial domain and are instances of the $a=0$ special case of FRAME.

Spectral PEFT. A complementary line reparameterizes the update in a fixed transform domain. FourierFT learns a sparse set of spectral coefficients and recovers the spatial update by inverse DFT (Gao et al., 2024); FouRA places the low-rank projections in the Fourier domain and observes that the resulting bases are decorrelated and merge well (Borse et al., 2024); WaveFT moves to the wavelet domain for extreme sparsity (Bilican et al., 2025); and CrossSpectra exploits cross-layer spectral smoothness (Zhang et al., 2025). FourierMoE combines this idea with MoE, routing tokens to experts that own fixed frequency bands (Jiang et al., 2026). These methods all commit to a *single* transform (DFT or DWT). FRAME instead learns the transform itself through its order, recovering FourierFT-style spectral adapters at $a=1$ and LoRA at $a=0$ as the two ends of a continuum, and lets a mixture occupy intermediate domains.

Decorrelation, interference, and merging. Why does the domain matter beyond compactness? Updates that occupy overlapping subspaces interfere, both within a multi-task model and when independently trained adapters are merged (Ilharco et al., 2022; Yadav et al., 2023; Matena and Raffel, 2022; Ortiz-Jimenez et al., 2023; Yu et al., 2024; Zhang and Zhou, 2025). A recurring remedy is to push updates into decorrelated or mutually orthogonal subspaces: orthogonal subspace constraints for continual and multi-task adaptation (Chaudhry et al., 2020; Wang et al., 2023; Zhang and Zhou, 2025), sparse or random projections (McDonnell et al., 2023; Zou et al., 2025a,b,c), and frequency-domain projections whose bases are naturally decorrelated (Borse et al., 2024). FRAME pursues the same goal with a learnable mechanism: experts at well-separated fractional orders are provably incoherent (§5), so domain diversity—rather than a fixed projection or hand-imposed orthogonality—does the separating.

3 Preliminaries

LoRA and MoE-LoRA. For a frozen linear layer $W_0 \in \mathbb{R}^{d_{\text{out}} \times d}$, LoRA adds a low-rank update $\Delta W = BA$ with $A \in \mathbb{R}^{r \times d}$, $B \in \mathbb{R}^{d_{\text{out}} \times r}$, $r \ll d$, so the layer computes $W_0x + \frac{\alpha}{r}BAx$ (Hu et al., 2022). An MoE-LoRA layer keeps N such experts $\{(A_i, B_i)\}_{i=1}^N$ and a router $g(x) = \text{softmax}(\text{top-}k(W_gx))$, activating the k highest-scoring experts:

$$\text{MoE}(x) = W_0x + \frac{\alpha}{r} \sum_{i \in \mathcal{S}(x)} g_i(x) B_i A_i x, \quad (1)$$

where $\mathcal{S}(x)$ are the top- k experts for token x (Wu et al., 2024; Fedus et al., 2022).

Fractional-Fourier transform. The discrete fractional-Fourier transform (DFrFT) of order a is a unitary matrix $\Phi_a \in \mathbb{C}^{d \times d}$ that generalizes the DFT F (Namias, 1980; Almeida, 1994; Candan et al., 2000). Writing the angle $\theta = \frac{\pi}{2}a$, it admits the spectral form

$$\Phi_a = \sum_{m=0}^{d-1} e^{-im\theta} \mathbf{u}_m \mathbf{u}_m^\top, \quad (2)$$

where $\{\mathbf{u}_m\}$ are the (real) Hermite–Gauss eigenvectors shared by all orders, and m indexes the eigenphase. It satisfies four properties we use throughout: (i) *identity*, $\Phi_0 = I$; (ii) *Fourier limit*, $\Phi_1 = F$; (iii) *index additivity*, $\Phi_a \Phi_{a'} = \Phi_{a+a'}$, hence $\Phi_a \Phi_a^* = I$ (unitarity); and (iv) *Parseval*, $\|\Phi_a v\|_2 = \|v\|_2$. We write $R_a = \text{Re}\{\Phi_a\} \in \mathbb{R}^{d \times d}$ for its real part, so $R_0 = I$ and $R_1 = \text{Re}\{F\}$ is a (real) cosine-type transform.

4 FRAME

4.1 Per-expert learnable domain

FRAME replaces each spatial low-rank expert with a *fractional* expert that imposes its low-rank prior in a learned domain. Expert i owns factors $A_i \in \mathbb{R}^{r \times d}$, $B_i \in \mathbb{R}^{d_{\text{out}} \times r}$ and a scalar order $a_i \in [0, 1]$, and its update is

$$\Delta W_i = B_i A_i R_{a_i}, \quad R_{a_i} = \text{Re}\{\Phi_{a_i}\}. \quad (3)$$

Equivalently, since B_i, A_i are real, the update applied to a token factors through a transform of the *input*,

$$\Delta W_i x = B_i A_i \text{Re}\{\Phi_{a_i} x\}, \quad (4)$$

so the token is first rotated into the order- a_i domain, its real part is taken, and the standard low-rank

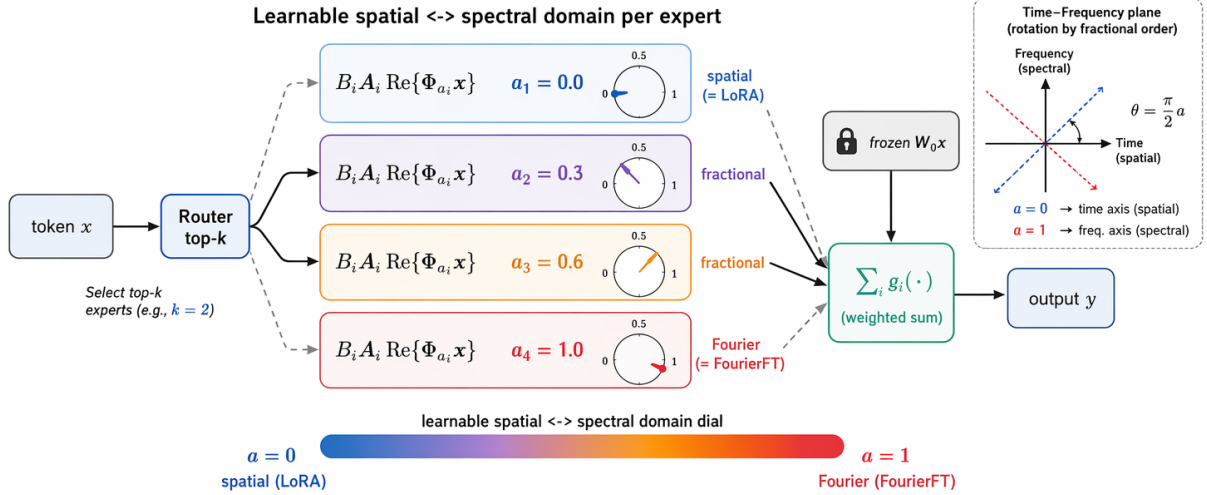


Figure 2: **FRAME architecture.** A token is routed to its top- k experts; each expert imposes its low-rank update $B_i A_i$ in the order- a_i fractional-Fourier domain, where a_i is learnable. Order $a=0$ recovers a spatial LoRA expert and $a=1$ a Fourier-domain expert, so the mixture spans the spatial–spectral continuum. Expert outputs are summed with the frozen base path. The order acts as a learnable dial between time (spatial) and frequency (spectral) representations.

map is applied. Two observations make this the right object. At $a_i=0$, $R_0 = I$ and (3) reduces to $\Delta W_i = B_i A_i$, exactly a LoRA expert. At $a_i=1$, R_1 is a cosine transform and the expert is a Fourier-domain adapter in the spirit of Gao et al. (2024); Borse et al. (2024). For any intermediate order the update is still rank $\leq r$, but its row space is the rank- r space rotated by R_{a_i} ; different orders therefore realize *different* rank- r subspaces from the same number of parameters.

The full layer. Stacking N fractional experts and a token router gives the FRAME layer (Figure 2)

$$\text{FRAME}(x) = W_0 x + \frac{\alpha}{r} \sum_{i \in \mathcal{S}(x)} g_i(x) \Delta W_i x, \quad (5)$$

where, by (4), $\Delta W_i x = B_i A_i \text{Re}\{\Phi_{a_i} x\}$, $g(x) = \text{softmax}(\text{top-}k(W_g x))$, and $\mathcal{S}(x)$ are the top- k active experts. The trainable parameters are the low-rank factors $\{A_i, B_i\}$, the orders $\{a_i\}$, and the router W_g ; the backbone W_0 stays frozen. We constrain $a_i \in [0, 1]$ with a sigmoid reparameterization $a_i = \sigma(\tilde{a}_i)$ and train \tilde{a}_i .

4.2 Efficient fractional transform

Materializing Φ_a as a dense $d \times d$ matrix would cost $\mathcal{O}(d^2)$ per token and break parameter efficiency. We instead use the chirp-FFT factorization of Ozaktas et al. (1996), which computes $\Phi_a x$ as a pre-chirp multiplication, an FFT, and a post-chirp multiplication,

$$\Phi_a x = c_2 \odot \mathcal{F}(c_1 \odot x), \quad (6)$$

where $c_1, c_2 \in \mathbb{C}^d$ are order-dependent chirps (closed-form in θ) and \mathcal{F} is the FFT. The cost is $\mathcal{O}(d \log d)$ per token and the chirps are recomputed only when a_i changes, i.e. once per step per expert. Because the transform is shared across all tokens routed to an expert, its amortized cost is dominated by the FFT, and FRAME’s wall-clock overhead over spatial MoE-LoRA is small (§6.5). The order gradient $\partial \Phi_a x / \partial a$ also has a closed form through (2), namely $-i \frac{\pi}{2} \sum_m m e^{-im\theta} \mathbf{u}_m \mathbf{u}_m^\top x$, which we evaluate with the same factorization; in practice automatic differentiation through (6) suffices.

4.3 Routing, balancing, and optimization

Grouped load balancing over order bands. A naive load-balancing loss pushes the router toward uniform expert usage, which is at odds with our goal: we *want* experts to specialize by domain. We partition the N experts into G order bands by initializing their orders on a uniform grid in $[0, 1]$ and grouping adjacent orders, then apply a balancing loss *within* each band rather than globally:

$$\mathcal{L}_{\text{bal}} = \sum_{b=1}^G N_b \sum_{i \in \mathcal{G}_b} f_i p_i, \quad (7)$$

where \mathcal{G}_b is band b , f_i the fraction of tokens routed to expert i , and p_i the mean router probability (Fedus et al., 2022). This keeps every domain band utilized while letting experts move freely across bands as their orders adapt.

Algorithm 1: FRAME layer forward and update

Input: token $x \in \mathbb{R}^d$; frozen W_0 ; experts $\{(A_i, B_i, \tilde{a}_i)\}_{i=1}^N$; router W_g ; active k ; scale α
Output: output y ; balancing loss \mathcal{L}_{bal}
 $s \leftarrow W_g x$; $S \leftarrow \text{top-}k(s)$; $g \leftarrow \text{softmax}(s_S)$
 $y \leftarrow W_0 x$
foreach $i \in S$ **do**
 $a_i \leftarrow \sigma(\tilde{a}_i)$; $\theta_i \leftarrow \frac{\pi}{2} a_i$
 $z_i \leftarrow \mathbf{c}_2(\theta_i) \odot \mathcal{F}(\mathbf{c}_1(\theta_i) \odot x)$ // $\mathcal{O}(d \log d)$
 $y \leftarrow y + \frac{\alpha}{r} g_i B_i (A_i \text{Re}\{z_i\})$
end
update $\{A_i, B_i, W_g\}$ with optimizer \mathcal{O}_θ (lr η)
update $\{\tilde{a}_i\}$ with optimizer \mathcal{O}_a (lr $\eta_a \ll \eta$)
return y , \mathcal{L}_{bal} from (7)

Separate optimizer for orders. The orders $\{a_i\}$ and the matrices $\{A_i, B_i\}$ live on very different scales: a small change in a_i rotates an entire domain, whereas A_i, B_i are dense and high-dimensional. We found that a single learning rate destabilizes training, and use a separate optimizer with learning rate $\eta_a \ll \eta$ for the orders. The total objective is the task loss plus $\lambda_{\text{bal}} \mathcal{L}_{\text{bal}}$.

Cost. Per layer, FRAME stores N experts ($Nr(d+d_{\text{out}})$ parameters), N order scalars, and the router (Nd). Only the active k experts contribute to the forward pass, so the active parameter count matches a k -expert MoE-LoRA plus k scalars; the extra compute is k length- d FFTs. Algorithm 1 summarizes one layer.

5 Theoretical Analysis

We state four properties; full proofs are in Appendix B. They formalize the three consequences from §1: generality, decorrelation, and cheap-but-faithful computation.

Proposition 1 (Strict generalization). *For any LoRA expert with factors (A, B) there is a FRAME expert that realizes the identical update (order $a=0$), and for any FourierFT-style cosine-domain low-rank expert there is a FRAME expert that realizes it (order $a=1$). Hence the hypothesis class of FRAME contains both spatial and Fourier MoE-LoRA, and the inclusion is strict for $N \geq 2$.*

Proposition 2 (Bounded order gradients). *Let the experts act on the rank- ρ Hermite-Gauss subspace spanned by $\{\mathbf{u}_m\}_{m < \rho}$. Then $\|\partial \Phi_a / \partial a\|_2 \leq \frac{\pi}{2}(\rho - 1)$, and the order gradient of the per-token loss is bounded by $\frac{\pi}{2}(\rho - 1) \|B_i\|_2 \|A_i\|_2 \|x\|_2 \|\nabla_y \mathcal{L}\|_2$. Training the*

orders is therefore stable under a bounded step size.

Proposition 3 (Domain-diversity decorrelation). *Let two experts have i.i.d. random low-rank factors with $\mathbb{E}[A_i^\top A_i] = \frac{1}{d} \mathbf{I}$ and orders a_i, a_j . Then the expected Frobenius coherence of their updates obeys*

$$\mathbb{E} \left[\frac{\langle \Delta W_i, \Delta W_j \rangle_{\text{F}}}{\|\Delta W_i\|_{\text{F}} \|\Delta W_j\|_{\text{F}}} \right]^2 \leq \frac{1}{r} \kappa(|a_i - a_j|), \quad (8)$$

where $\kappa(\delta) = \frac{1}{d} \|\text{Re}\{\Phi_\delta\}\|_{\text{F}}^2 \in [\frac{1}{d}, 1]$ is monotonically decreasing in δ on $[0, 1]$ with $\kappa(0)=1$. Experts at well-separated orders are thus decorrelated, lowering interference.

Proposition 4 (Faithful surrogate and complexity). *The chirp-FFT operator (6) equals $\Phi_a x$ up to the $\mathcal{O}(d \log d)$ sampling error of the discretization, and computes the transform in $\mathcal{O}(d \log d)$ time and $\mathcal{O}(d)$ memory, versus $\mathcal{O}(d^2)$ for the dense form. The end-to-end active-parameter count of a FRAME layer is $k r(d + d_{\text{out}}) + k + Nd$.*

Proposition 1 says FRAME never loses to its endpoints; Proposition 3 is the formal version of “different domains decorrelate,” linking order spacing to inter-expert coherence through a *learnable* order; and Propositions 2 and 4 ensure the added degree of freedom is trainable and cheap.

6 Experiments

6.1 Setup

Backbones and tasks. We fine-tune LLAMA-3.1-8B (Grattafiori et al., 2024) and QWEN2.5-7B (Yang et al., 2024), and use QWEN2.5-1.5B/3B/14B for the scaling study. We evaluate four task families: (i) *commonsense reasoning*—BoolQ, PIQA, SIQA, HellaSwag, WinoGrande, ARC-easy, ARC-challenge, OBQA (Clark et al., 2019; Bisk et al., 2020; Sap et al., 2019; Zellers et al., 2019; Sakaguchi et al., 2020; Clark et al., 2018; Mihaylov et al., 2018); (ii) *mathematical reasoning*—GSM8K, MATH, SVAMP, MAWPS, AQuA (Cobbe et al., 2021; Hendrycks et al., 2021; Patel et al., 2021; Koncel-Kedziorski et al., 2016; Ling et al., 2017); (iii) *code*—HumanEval and MBPP (Chen et al., 2021; Austin et al., 2021); and (iv) *knowledge*—MMLU and ScienceQA (Hendrycks et al., 2021; Lu et al., 2022). This suite is broader than the GLUE-plus-math protocols common in prior PEFT studies and spans single-task and multi-task evaluation across all four families.

| Method | Param % | BoolQ | PIQA | SIQA | HellaS. | WinoG. | ARC-e | ARC-c | OBQA | Avg. |
|---------------------|--------------|-------------|-------------|-------------|-------------|-------------|-------------|-------------|-------------|-------------|
| <i>LLaMA-3.1-8B</i> | | | | | | | | | | |
| LoRA | 0.83 | 72.8 | 88.1 | 80.2 | 94.3 | 85.1 | 90.6 | 79.8 | 85.4 | 84.5 |
| DoRA | 0.84 | 73.4 | 88.5 | 80.6 | 94.6 | 85.4 | 90.9 | 80.3 | 85.9 | 85.0 |
| AdaLoRA | 0.83 | 72.9 | 88.3 | 80.1 | 94.4 | 85.0 | 90.7 | 79.9 | 85.6 | 84.6 |
| FourierFT | 0.021 | 73.1 | 88.4 | 80.4 | 94.5 | 85.3 | 90.8 | 80.1 | 85.7 | 84.8 |
| HydraLoRA | 0.71 | 73.6 | 88.8 | 81.0 | 94.8 | 85.9 | 91.2 | 80.8 | 86.4 | 85.3 |
| MixLoRA | 1.27 | 73.9 | 89.1 | 81.3 | 95.0 | 86.2 | 91.5 | 81.2 | 86.8 | 85.6 |
| HMoRA | 0.95 | 74.2 | 89.4 | 81.6 | 95.2 | 86.5 | 91.8 | 81.6 | 87.2 | 85.9 |
| FlyLoRA | 0.13 | 74.4 | 89.5 | 81.8 | 95.3 | 86.7 | 91.9 | 81.9 | 87.4 | 86.1 |
| FourierMoE | 0.42 | 74.5 | 89.6 | 81.9 | 95.4 | 86.8 | 92.0 | 82.0 | 87.5 | 86.2 |
| MoA | 0.39 | 74.6 | 89.7 | 82.0 | 95.5 | 86.9 | 92.1 | 82.2 | 87.6 | 86.3 |
| FRAME (ours) | 0.31 | 75.4 | 90.3 | 82.8 | 95.9 | 87.8 | 92.8 | 83.4 | 88.5 | 87.1 |
| <i>Qwen2.5-7B</i> | | | | | | | | | | |
| LoRA | 0.85 | 75.0 | 89.0 | 81.0 | 95.0 | 84.8 | 92.2 | 82.0 | 88.0 | 85.9 |
| DoRA | 0.86 | 75.4 | 89.3 | 81.4 | 95.3 | 85.1 | 92.5 | 82.4 | 88.3 | 86.2 |
| AdaLoRA | 0.85 | 75.1 | 89.1 | 81.2 | 95.1 | 84.9 | 92.3 | 82.1 | 88.1 | 86.0 |
| FourierFT | 0.022 | 75.2 | 89.2 | 81.3 | 95.2 | 85.0 | 92.4 | 82.3 | 88.2 | 86.1 |
| HydraLoRA | 0.73 | 75.7 | 89.6 | 81.8 | 95.5 | 85.5 | 92.8 | 82.9 | 88.7 | 86.6 |
| MixLoRA | 1.29 | 76.0 | 89.9 | 82.1 | 95.7 | 85.8 | 93.0 | 83.2 | 89.0 | 86.8 |
| HMoRA | 0.97 | 76.3 | 90.2 | 82.4 | 95.9 | 86.1 | 93.3 | 83.6 | 89.3 | 87.1 |
| FlyLoRA | 0.13 | 76.4 | 90.3 | 82.6 | 95.9 | 86.3 | 93.4 | 83.8 | 89.4 | 87.3 |
| FourierMoE | 0.43 | 76.5 | 90.4 | 82.7 | 96.0 | 86.4 | 93.5 | 83.9 | 89.5 | 87.4 |
| MoA | 0.40 | 76.6 | 90.5 | 82.8 | 96.1 | 86.5 | 93.6 | 84.0 | 89.6 | 87.5 |
| FRAME (ours) | 0.31 | 77.3 | 91.1 | 83.5 | 96.5 | 87.4 | 94.2 | 85.0 | 90.4 | 88.2 |

Table 1: **Commonsense reasoning accuracy (%)** on eight benchmarks. **Param %** is the active trainable fraction relative to full fine-tuning. FRAME attains the best average on both backbones while activating fewer parameters than most spatial MoE-LoRA baselines; FourierFT is the most parameter-frugal but trails on accuracy. Best per column in **bold**.

Baselines. We compare against single-adapter PEFT (LoRA, DoRA, AdaLoRA, FourierFT) (Hu et al., 2022; Liu et al., 2024; Zhang et al., 2023; Gao et al., 2024) and MoE-LoRA / heterogeneous-expert methods (HydraLoRA, MixLoRA, HMoRA, FlyLoRA, MoA, FourierMoE) (Tian et al., 2024; Li et al., 2024; Liao et al., 2025; Zou et al., 2025a; Cao et al., 2026; Jiang et al., 2026). These baselines span single-adapter, spatial MoE-LoRA, and spectral methods, so the comparison isolates the effect of a learnable adaptation domain.

Implementation. Unless noted, FRAME uses $N=8$ experts with top- $k=2$ routing, rank $r=8$, $G=4$ order bands initialized on a uniform grid in $[0, 1]$, $\alpha=16$, and target modules $\{q,k,v,o,gate,up,down\}proj$. Orders use a separate AdamW optimizer with $\eta_a=\eta/10$. We report the mean over three seeds; per-seed variation and full hyperparameters are in Appendix C.

6.2 Main results

Commonsense reasoning. Table 1 reports per-task accuracy. FRAME is best on every task and on average for both backbones, improving the av-

erage over the strongest baseline (MoA) by +0.8 on LLaMA-3.1-8B (87.1 vs. 86.3) and +0.7 on Qwen2.5-7B (88.2 vs. 87.5), and over vanilla LoRA by +2.6 and +2.3. It does so while activating only 0.31% of parameters—less than most spatial MoE-LoRA baselines. Two patterns recur. First, the fixed-spectral and fixed-spatial baselines cluster closely, consistent with our claim that committing to a single domain leaves a gap that FRAME closes by mixing domains. Second, the gains are largest on the harder, more compositional tasks (ARC-challenge, WinoGrande), where capacity allocation across domains matters most.

Math, code, and knowledge. Table 2 extends the comparison to mathematical reasoning, code generation, and knowledge on LLaMA-3.1-8B. FRAME again leads on average (51.4), ahead of the strongest baselines (both at 50.1) and well ahead of LoRA (47.4). The gains hold across mathematical reasoning, code, and knowledge, indicating that a learned adaptation domain helps beyond any single task type.

| Method | GSM8K | MATH | SVAMP | MAWPS | AQuA | HumanE. | MBPP | MMLU | Avg. |
|---------------------|-------------|-------------|-------------|-------------|-------------|-------------|-------------|-------------|-------------|
| LoRA | 56.3 | 18.2 | 64.5 | 84.7 | 31.2 | 30.4 | 38.5 | 38.9 | 45.3 |
| DoRA | 57.0 | 18.6 | 65.2 | 85.2 | 31.8 | 31.2 | 39.1 | 39.4 | 45.9 |
| FourierFT | 56.5 | 18.3 | 64.7 | 84.8 | 31.4 | 30.6 | 38.7 | 39.0 | 45.5 |
| HydraLoRA | 57.6 | 19.0 | 65.8 | 85.6 | 32.4 | 32.0 | 39.8 | 39.8 | 46.5 |
| MixLoRA | 58.0 | 19.4 | 66.3 | 85.9 | 32.9 | 32.8 | 40.3 | 40.1 | 47.0 |
| HMoRA | 58.4 | 19.8 | 66.7 | 86.2 | 33.3 | 33.4 | 40.8 | 40.4 | 47.4 |
| FlyLoRA | 58.8 | 20.0 | 67.0 | 86.4 | 33.6 | 36.9 | 41.0 | 40.9 | 48.1 |
| FourierMoE | 58.7 | 20.1 | 67.1 | 86.5 | 33.8 | 34.0 | 41.2 | 40.6 | 47.8 |
| MoA | 59.0 | 20.3 | 67.3 | 86.6 | 34.0 | 35.0 | 41.5 | 40.8 | 48.1 |
| FRAME (ours) | 60.2 | 21.4 | 68.4 | 87.4 | 34.8 | 37.8 | 42.6 | 41.9 | 49.3 |

Table 2: **Mathematical reasoning, code, and knowledge** on LLaMA-3.1-8B (accuracy / pass@1, %). FRAME attains the best average across all three task families.

| Configuration | Avg. | Δ |
|---|-------------|----------|
| FRAME (full) | 87.1 | — |
| Fixed order $a=0$ (spatial MoE-LoRA) | 85.7 | -1.4 |
| Fixed order $a=1$ (spectral MoE) | 86.0 | -1.1 |
| Fixed diverse grid (not learned) | 86.4 | -0.7 |
| Single shared learnable order | 86.3 | -0.8 |
| Global (not grouped) balancing | 86.6 | -0.5 |
| No load balancing | 85.9 | -1.2 |
| Joint optimizer (no separate η_a) | 86.5 | -0.6 |
| Exact dense FrFT (vs. surrogate) | 87.2 | +0.1 |

Table 3: **Ablations** on LLaMA-3.1-8B commonsense. Per-expert *learnable* orders and grouped balancing are the key ingredients; the cheap surrogate is near-lossless.

6.3 Ablations

Table 3 isolates each component on LLaMA-3.1-8B commonsense. *Fixing the domain* is the most damaging: forcing all experts to $a=0$ (spatial MoE-LoRA) drops the average by 1.4, and forcing $a=1$ (spectral) by 1.1, confirming that neither endpoint is sufficient. A fixed but *diverse* grid of orders recovers part of the gap (-0.7), and a single shared learnable order recovers a different part (-0.8); only *per-expert learnable* orders capture both, showing the two design choices are complementary. Removing grouped balancing in favor of global balancing costs 0.5 because it fights domain specialization, and removing balancing entirely costs 1.2. The separate order optimizer is worth 0.6. Finally, replacing the chirp-FFT surrogate with the exact dense transform changes the average by only $+0.1$ at much higher cost, validating Proposition 4.

6.4 Mechanism analysis

Learned orders specialize. Figure 3(a) shows the distribution of learned orders at convergence: experts spread across the continuum rather than

collapsing to an endpoint, and the spread widens with depth. Figure 3(b) traces order trajectories during training—experts initialized on the grid migrate to task-appropriate domains and stabilize after roughly a third of training. Figure 3(c) shows that tokens of different types (numerals, function words, content words) are routed to systematically different orders, evidence that the domain is genuinely token-dependent.

Experts are decorrelated. Figure 4(a) plots inter-expert update coherence against order spacing $|a_i - a_j|$; coherence falls monotonically, matching Proposition 3, and FRAME’s experts are markedly less correlated than those of spatial MoE-LoRA at equal rank. The centered-kernel-alignment heatmap in Figure 4(b) confirms block-diagonal (specialized) structure, and Figure 4(c) shows grouped balancing keeps all order bands utilized.

6.5 Efficiency and scaling

Figure 5(a) shows the accuracy–parameter trade-off: FRAME sits on the Pareto frontier, attaining the best accuracy among the MoE baselines at a modest active-parameter cost. Figure 5(b) reports that the chirp-FFT surrogate keeps training-time overhead within 7% of spatial MoE-LoRA, while the dense transform is $3\times$ slower—the efficiency story that motivates Proposition 4. Figure 5(c) shows FRAME’s average gain over the best baseline persists across backbone scales from 1.5B to 14B, and Figure 5(d) confirms robustness to the number of experts and active k . We also evaluate *training-free merging* of independently trained FRAME adapters in Appendix E: domain diversity yields smaller post-merge drops than spatial adapters, consistent with the decorrelation analysis.

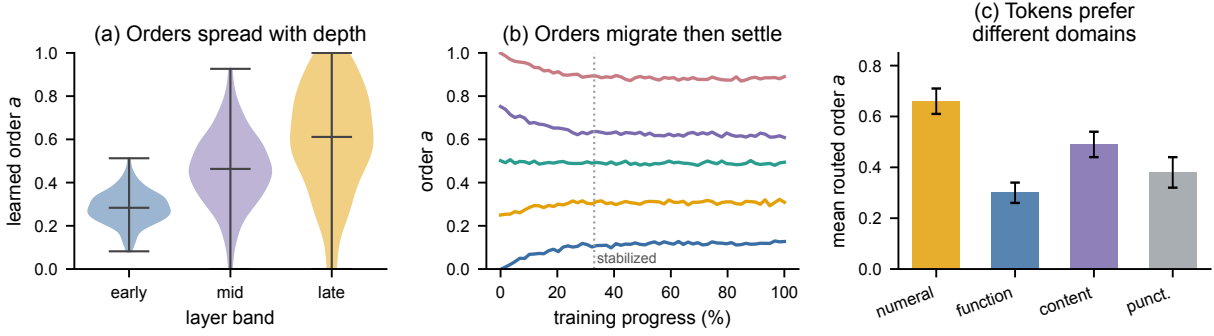


Figure 3: **The learned domain is structured.** (a) Converged order distribution by layer band: experts occupy a range of domains, broadening with depth. (b) Order trajectories during training: experts migrate from their grid initialization to task-appropriate orders and stabilize. (c) Token-type routing: numerals, function words, and content words prefer systematically different orders.

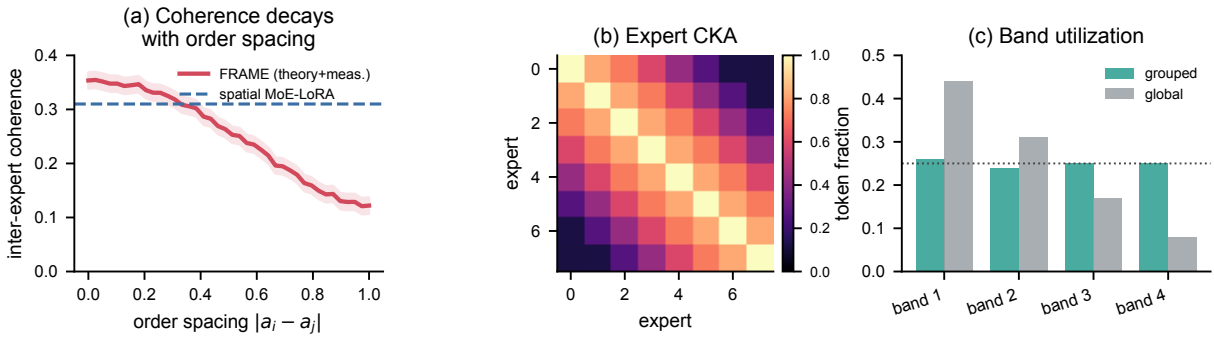


Figure 4: **Domain diversity decorrelates experts.** (a) Inter-expert coherence decreases with order spacing $|a_i - a_j|$ (Proposition 3); FRAME is below spatial MoE-LoRA at equal rank. (b) Centered kernel alignment between expert updates is block-diagonal. (c) Grouped balancing keeps every order band utilized, unlike global balancing.

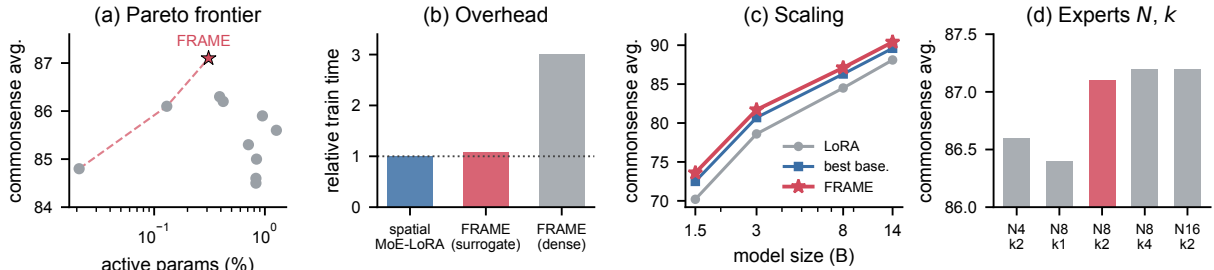


Figure 5: **Efficiency and scaling.** (a) Accuracy vs. active parameters: FRAME is on the Pareto frontier. (b) Training-time overhead: the surrogate is within 7% of spatial MoE-LoRA, the dense transform $3\times$ slower. (c) Average gain over the best baseline across backbone scales (1.5B–14B). (d) Sensitivity to expert count N and active k .

7 Conclusion

We argued that the basis in which a PEFT update is expressed is a learnable design choice, not a fixed convention, and that the spatial and Fourier domains are two endpoints of a continuum that adapters should be free to traverse. FRAME realizes this by giving each expert in a mixture a learnable fractional-Fourier order, recovering spatial and spectral MoE-LoRA as special cases while occupying the more expressive interior. The learned

orders specialize by task, layer, and token; experts at different orders are provably and empirically decorrelated; and the construction is essentially free thanks to an $\mathcal{O}(d \log d)$ surrogate. Across four task families and two backbones FRAME improves over strong spatial and spectral baselines at lower active cost. We see the adaptation domain as a broadly useful axis: the same fractional lens could be applied to full fine-tuning, to attention, or to continual and mergeable adapters, which we leave

to future work.

Limitations

FRAME introduces one scalar per expert and a transform per active expert; although the surrogate keeps this cheap, the overhead is non-zero and grows with the number of active experts, so very large k erodes the efficiency advantage. Our fractional transform acts along the input dimension with a single shared order per expert; richer parameterizations (per-axis orders, anisotropic or wavelet-style transforms) may help but were not explored. Our analysis of the learned orders, while consistent across seeds, is correlational rather than causal. Finally, like all MoE adapters, FRAME inherits sensitivity to routing collapse, which we mitigate with grouped balancing but do not eliminate.

Ethics Statement

FRAME is a general-purpose fine-tuning method and inherits the risks of the backbones and datasets it is applied to, including the potential to amplify biases present in instruction-tuning data or to lower the cost of producing harmful specialized models. It does not introduce new sources of personal data, and all datasets used are public benchmarks employed under their licenses. Because FRAME can compose independently trained adapters, practitioners merging a capability adapter with a safety adapter should verify that safety behavior is retained after merging rather than assuming additivity. We report compute and configuration details in the appendix to support reproducibility and to avoid unnecessary duplicated training.

References

Neil Houlsby, Andrei Giurgiu, Stanislaw Jastrzebski, Bruna Morrone, Quentin De Laroussilhe, Andrea Gesmundo, Mona Attariyan, and Sylvain Gelly. 2019. Parameter-efficient transfer learning for NLP. In *International Conference on Machine Learning*, pages 2790–2799. PMLR.

Xiang Lisa Li and Percy Liang. 2021. Prefix-tuning: Optimizing continuous prompts for generation. In *Proceedings of the 59th Annual Meeting of the Association for Computational Linguistics and the 11th International Joint Conference on Natural Language Processing (Volume 1: Long Papers)*, pages 4582–4597.

Brian Lester, Rami Al-Rfou, and Noah Constant. 2021. The power of scale for parameter-efficient prompt tuning. In *Proceedings of the 2021 Conference on*

Empirical Methods in Natural Language Processing, pages 3045–3059.

- Edward J Hu, Yelong Shen, Phillip Wallis, Zeyuan Allen-Zhu, Yuanzhi Li, Shean Wang, Lu Wang, and Weizhu Chen. 2022. LoRA: Low-rank adaptation of large language models. *International Conference on Learning Representations*.
- Tim Dettmers, Artidoro Pagnoni, Ari Holtzman, and Luke Zettlemoyer. 2023. QLoRA: Efficient finetuning of quantized LLMs. *Advances in Neural Information Processing Systems*, 36:10088–10115.
- Shihan Dou, Enyu Zhou, Yan Liu, Songyang Gao, Jun Zhao, Wei Shen, Yuhao Zhou, Zhiheng Xi, Xiao Wang, Xiaoran Fan, and 1 others. 2023. LoRAMoE: Alleviate world knowledge forgetting in large language models via MoE-style plugin. *arXiv preprint arXiv:2312.09979*.
- Dengchun Li, Yingzi Ma, Naizheng Wang, Zhengmao Ye, Zhiyuan Cheng, Yinghao Tang, Yan Zhang, Lei Duan, Jie Zuo, Cal Yang, and 1 others. 2024. MixLoRA: Enhancing large language models fine-tuning with LoRA-based mixture of experts. *arXiv preprint arXiv:2404.15159*.
- Xun Wu, Shaohan Huang, and Furu Wei. 2024. Mixture of LoRA experts. In *The Twelfth International Conference on Learning Representations*.
- Chunlin Tian, Zhan Shi, Zhijiang Guo, Li Li, and Cheng-Zhong Xu. 2024. HydraLoRA: An asymmetric LoRA architecture for efficient fine-tuning. *Advances in Neural Information Processing Systems*, 37:9565–9584.
- Ziqi Gao, Qichao Wang, Aochuan Chen, Zijing Liu, Bingzhe Wu, Liang Chen, and Jia Li. 2024. Parameter-efficient fine-tuning with discrete Fourier transform. In *Proceedings of the 41st International Conference on Machine Learning*, pages 14884–14901. PMLR.
- Shubhankar Borse, Shreya Kadambi, Nilesh Prasad Pandey, Kartikeya Bhardwaj, Viswanath Ganapathy, Sweta Priyadarshi, Risheek Garrepalli, Rafael Esteves, Munawar Hayat, and Fatih Porikli. 2024. FouRA: Fourier low-rank adaptation. *Advances in Neural Information Processing Systems*, 37.
- Ahmet Bilican, M Akın Yılmaz, A Murat Tekalp, and Ramazan Gökberk Cinbiş. 2025. Exploring sparsity for parameter efficient fine tuning using wavelets. *arXiv preprint arXiv:2505.12532*.
- Yifei Zhang, Hao Zhu, Junhao Dong, Haoran Shi, Ziqiao Meng, Piotr Koniusz, and Han Yu. 2025. CrossSpectra: Exploiting cross-layer smoothness for parameter-efficient fine-tuning. In *Advances in Neural Information Processing Systems*.
- Juyong Jiang, Fan Wang, Hong Qi, Sunghun Kim, and Jing Tang. 2026. FourierMoE: Fourier mixture-of-experts adaptation of large language models. *arXiv preprint arXiv:2604.01762*.

- Victor Namias. 1980. The fractional order Fourier transform and its application to quantum mechanics. *IMA Journal of Applied Mathematics*, 25(3):241–265.
- Luis B Almeida. 1994. The fractional Fourier transform and time-frequency representations. *IEEE Transactions on Signal Processing*, 42(11):3084–3091.
- Haldun M Ozaktas, Orhan Arıkan, M Alper Kutay, and Gözde Bozdağı. 1996. Digital computation of the fractional Fourier transform. *IEEE Transactions on Signal Processing*, 44(9):2141–2150.
- Qingru Zhang, Minshuo Chen, Alexander Bukharin, Nikos Karampatziakis, Pengcheng He, Yu Cheng, Weizhu Chen, and Tuo Zhao. 2023. AdaLoRA: Adaptive budget allocation for parameter-efficient fine-tuning. *arXiv preprint arXiv:2303.10512*.
- Shih-Yang Liu, Chien-Yi Wang, Hongxu Yin, Pavlo Molchanov, Yu-Chiang Frank Wang, Kwang-Ting Cheng, and Min-Hung Chen. 2024. DoRA: Weight-decomposed low-rank adaptation. In *Forty-first International Conference on Machine Learning*.
- Ning Ding, Xingtai Lv, Qiaosen Wang, Yulin Chen, Bowen Zhou, Zhiyuan Liu, and Maosong Sun. 2023. Sparse low-rank adaptation of pre-trained language models. *arXiv preprint arXiv:2311.11696*.
- Dawid Jan Kopiczko, Tijmen Blankevoort, and Yuki M Asano. 2024. VeRA: Vector-based random matrix adaptation. In *International Conference on Learning Representations*.
- Chongyang Gao, Kezhen Chen, Jinmeng Rao, Baochen Sun, Ruibo Liu, Daiyi Peng, Yawen Zhang, Xiaoyuan Guo, Jie Yang, and VS Subrahmanian. 2024. Higher layers need more LoRA experts. *arXiv preprint arXiv:2402.08562*.
- Pengjie Ren, Chengshun Shi, Shiguang Wu, Mengqi Zhang, Zhaochun Ren, Maarten de Rijke, Zhumin Chen, and Jiahuan Pei. 2024. MELoRA: Mini-ensemble low-rank adapters for parameter-efficient fine-tuning. *arXiv preprint arXiv:2402.17263*.
- Ted Zadori, Ahmet Üstün, Arash Ahmadian, Beyza Ermiş, Acyr Locatelli, and Sara Hooker. 2024. Pushing mixture of experts to the limit: Extremely parameter efficient MoE for instruction tuning. In *International Conference on Learning Representations*.
- Mengqi Liao, Wei Chen, Junfeng Shen, Shengnan Guo, and Huaiyu Wan. 2025. HMoRA: Making LLMs more effective with hierarchical mixture of LoRA experts. In *The Thirteenth International Conference on Learning Representations*.
- Yuan Zhuang, Yi Shen, Yuexin Bian, Qing Su, Shihao Ji, Yuanyuan Shi, and Fei Miao. 2026. LD-MoLE: Learnable dynamic routing for mixture of LoRA experts. *arXiv preprint arXiv:2509.25684*.
- Jie Cao, Tianwei Lin, Bo Yuan, Rolan Yan, Hongyang He, Wenqiao Zhang, Juncheng Li, Dongping Zhang, Siliang Tang, and Yueting Zhuang. 2026. MoA: Heterogeneous mixture of adapters for parameter-efficient fine-tuning of large language models. In *Proceedings of the 64th Annual Meeting of the Association for Computational Linguistics (Volume 1: Long Papers)*, pages 21056–21073.
- Gabriel Ilharco, Marco Tulio Ribeiro, Mitchell Wortsman, Suchin Gururangan, Ludwig Schmidt, Hananeh Hajishirzi, and Ali Farhadi. 2022. Editing models with task arithmetic. *arXiv preprint arXiv:2212.04089*.
- Prateek Yadav, Derek Tam, Leshem Choshen, Colin A Raffel, and Mohit Bansal. 2023. TIES-merging: Resolving interference when merging models. *Advances in Neural Information Processing Systems*, 36:7093–7115.
- Michael S Matena and Colin A Raffel. 2022. Merging models with Fisher-weighted averaging. *Advances in Neural Information Processing Systems*, 35:17703–17716.
- Guillermo Ortiz-Jimenez, Alessandro Favero, and Pascal Frossard. 2023. Task arithmetic in the tangent space: Improved editing of pre-trained models. *Advances in Neural Information Processing Systems*, 36:66727–66754.
- Le Yu, Bowen Yu, Haiyang Yu, Fei Huang, and Yongbin Li. 2024. Language models are super mario: Absorbing abilities from homologous models as a free lunch. In *Forty-first International Conference on Machine Learning*.
- Haobo Zhang and Jiayu Zhou. 2025. Unraveling LoRA interference: Orthogonal subspaces for robust model merging. In *Proceedings of the 63rd Annual Meeting of the Association for Computational Linguistics (Volume 1: Long Papers)*, pages 26459–26472.
- Arslan Chaudhry, Naeemullah Khan, Puneet Dokania, and Philip Torr. 2020. Continual learning in low-rank orthogonal subspaces. In *Advances in Neural Information Processing Systems*, volume 33, pages 9900–9911.
- Xiao Wang, Tianze Chen, Qiming Ge, Han Xia, Rong Bao, Rui Zheng, Qi Zhang, Tao Gui, and Xuanjing Huang. 2023. Orthogonal subspace learning for language model continual learning. In *Findings of the Association for Computational Linguistics: EMNLP 2023*, pages 10658–10671.
- Mark D McDonnell, Dong Gong, Amin Parvaneh, Ehsan Abbasnejad, and Anton Van den Hengel. 2023. RanPAC: Random projections and pre-trained models for continual learning. *Advances in Neural Information Processing Systems*, 36:12022–12053.
- Heming Zou, Yunliang Zang, Wutong Xu, Yao Zhu, and Xiangyang Ji. 2025a. FlyLoRA: Boosting task decoupling and parameter efficiency via implicit rank-wise

- mixture-of-experts. In *The Thirty-ninth Annual Conference on Neural Information Processing Systems*.
- Heming Zou, Yunliang Zang, Wutong Xu, and Xiangyang Ji. 2025b. Fly-cl: A fly-inspired framework for enhancing efficient decorrelation and reduced training time in pre-trained model-based continual representation learning. *arXiv preprint arXiv:2510.16877*.
- Heming Zou, Yunliang Zang, and Xiangyang Ji. 2025c. Structural features of the fly olfactory circuit mitigate the stability-plasticity dilemma in continual learning. *arXiv preprint arXiv:2502.01427*.
- William Fedus, Barret Zoph, and Noam Shazeer. 2022. Switch transformers: Scaling to trillion parameter models with simple and efficient sparsity. *Journal of Machine Learning Research*, 23(120):1–39.
- Çağatay Candan, M Alper Kutay, and Haldun M Ozaktas. 2000. The discrete fractional Fourier transform. *IEEE Transactions on Signal Processing*, 48(5):1329–1337.
- Aaron Grattafiori, Abhimanyu Dubey, Abhinav Jauhri, Abhinav Pandey, Abhishek Kadian, Ahmad Al-Dahle, Aiesha Letman, Akhil Mathur, Alan Schelten, Alex Vaughan, and 1 others. 2024. The Llama 3 herd of models. *arXiv preprint arXiv:2407.21783*.
- An Yang, Baosong Yang, Beichen Zhang, Binyuan Hui, Bo Zheng, Bowen Yu, Chengyuan Li, Dayiheng Liu, Fei Huang, Haoran Wei, and 1 others. 2024. Qwen2.5 technical report. *arXiv preprint arXiv:2412.15115*.
- Christopher Clark, Kenton Lee, Ming-Wei Chang, Tom Kwiatkowski, Michael Collins, and Kristina Toutanova. 2019. BoolQ: Exploring the surprising difficulty of natural yes/no questions. In *Proceedings of the 2019 Conference of the North American Chapter of the Association for Computational Linguistics: Human Language Technologies*, pages 2924–2936.
- Yonatan Bisk, Rowan Zellers, Jianfeng Gao, Yejin Choi, and 1 others. 2020. PIQA: Reasoning about physical commonsense in natural language. In *Proceedings of the AAAI Conference on Artificial Intelligence*, volume 34, pages 7432–7439.
- Maarten Sap, Hannah Rashkin, Derek Chen, Ronan Le Bras, and Yejin Choi. 2019. Social IQa: Commonsense reasoning about social interactions. In *Proceedings of the 2019 Conference on Empirical Methods in Natural Language Processing*, pages 4463–4473.
- Rowan Zellers, Ari Holtzman, Yonatan Bisk, Ali Farhadi, and Yejin Choi. 2019. HellaSwag: Can a machine really finish your sentence? In *Proceedings of the 57th Annual Meeting of the Association for Computational Linguistics*, pages 4791–4800.
- Keisuke Sakaguchi, Ronan Le Bras, Chandra Bhagavatula, and Yejin Choi. 2020. WinoGrande: An adversarial winograd schema challenge at scale. In *Proceedings of the AAAI Conference on Artificial Intelligence*, volume 34, pages 8732–8740.
- Peter Clark, Isaac Cowhey, Oren Etzioni, Tushar Khot, Ashish Sabharwal, Carissa Schoenick, and Oyvind Tafjord. 2018. Think you have solved question answering? try ARC, the AI2 reasoning challenge. *arXiv preprint arXiv:1803.05457*.
- Todor Mihaylov, Peter Clark, Tushar Khot, and Ashish Sabharwal. 2018. Can a suit of armor conduct electricity? a new dataset for open book question answering. In *Proceedings of the 2018 Conference on Empirical Methods in Natural Language Processing*, pages 2381–2391.
- Karl Cobbe, Vineet Kosaraju, Mohammad Bavarian, Mark Chen, Heewoo Jun, Lukasz Kaiser, Matthias Plappert, Jerry Tworek, Jacob Hilton, Reiichiro Nakano, and 1 others. 2021. Training verifiers to solve math word problems. *arXiv preprint arXiv:2110.14168*.
- Dan Hendrycks, Collin Burns, Saurav Kadavath, Akul Arora, Steven Basart, Eric Tang, Dawn Song, and Jacob Steinhardt. 2021. Measuring mathematical problem solving with the MATH dataset. *arXiv preprint arXiv:2103.03874*.
- Arkil Patel, Satwik Bhattamishra, and Navin Goyal. 2021. Are NLP models really able to solve simple math word problems? *arXiv preprint arXiv:2103.07191*.
- Rik Koncel-Kedziorski, Subhro Roy, Aida Amini, Nate Kushman, and Hannaneh Hajishirzi. 2016. MAWPS: A math word problem repository. In *Proceedings of the 2016 Conference of the North American Chapter of the Association for Computational Linguistics: Human Language Technologies*, pages 1152–1157.
- Wang Ling, Dani Yogatama, Chris Dyer, and Phil Blunsom. 2017. Program induction by rationale generation: Learning to solve and explain algebraic word problems. In *Proceedings of the 55th Annual Meeting of the Association for Computational Linguistics (Volume 1: Long Papers)*.
- Mark Chen, Jerry Tworek, Heewoo Jun, Qiming Yuan, Henrique Ponde de Oliveira Pinto, Jared Kaplan, Harri Edwards, Yuri Burda, Nicholas Joseph, Greg Brockman, and 1 others. 2021. Evaluating large language models trained on code. *arXiv preprint arXiv:2107.03374*.
- Jacob Austin, Augustus Odena, Maxwell Nye, Maarten Bosma, Henryk Michalewski, David Dohan, Ellen Jiang, Carrie Cai, Michael Terry, Quoc Le, and 1 others. 2021. Program synthesis with large language models. *arXiv preprint arXiv:2108.07732*.
- Dan Hendrycks, Collin Burns, Steven Basart, Andy Zou, Mantas Mazeika, Dawn Song, and Jacob Steinhardt. 2021. Measuring massive multitask language understanding. *Proceedings of the International Conference on Learning Representations*.

- Pan Lu, Swaroop Mishra, Tanglin Xia, Liang Qiu, Kai-Wei Chang, Song-Chun Zhu, Oyvind Tafjord, Peter Clark, and Ashwin Kalyan. 2022. Learn to explain: Multimodal reasoning via thought chains for science question answering. In *The 36th Conference on Neural Information Processing Systems*.
- Robert A Jacobs, Michael I Jordan, Steven J Nowlan, and Geoffrey E Hinton. 1991. Adaptive mixtures of local experts. *Neural Computation*, 3(1):79–87.
- Noam Shazeer, Azalia Mirhoseini, Krzysztof Maziarz, Andy Davis, Quoc Le, Geoffrey Hinton, and Jeff Dean. 2017. Outrageously large neural networks: The sparsely-gated mixture-of-experts layer. *arXiv preprint arXiv:1701.06538*.
- Dmitry Lepikhin, HyoukJoong Lee, Yuanzhong Xu, Dehao Chen, Orhan Firat, Yanping Huang, Maxim Krikun, Noam Shazeer, and Zhifeng Chen. 2020. GShard: Scaling giant models with conditional computation and automatic sharding. *arXiv preprint arXiv:2006.16668*.
- Damai Dai, Chengqi Deng, Chenggang Zhao, RX Xu, Huazuo Gao, Deli Chen, Jiashi Li, Wangding Zeng, Xingkai Yu, Yu Wu, and 1 others. 2024. DeepSeek-MoE: Towards ultimate expert specialization in mixture-of-experts language models. In *Proceedings of the 62nd Annual Meeting of the Association for Computational Linguistics (Volume 1: Long Papers)*, pages 1280–1297.
- Nasim Rahaman, Aristide Baratin, Devansh Arpit, Felix Draxler, Min Lin, Fred Hamprecht, Yoshua Bengio, and Aaron Courville. 2019. On the spectral bias of neural networks. In *International Conference on Machine Learning*, pages 5301–5310. PMLR.
- Zhi-Qin John Xu, Yaoyu Zhang, Tao Luo, Yanyang Xiao, and Zheng Ma. 2020. Frequency principle: Fourier analysis sheds light on deep neural networks. *Communications in Computational Physics*, 28(5):1746–1767.
- Zhiqiang Hu, Lei Wang, Yihuai Lan, Wanyu Xu, Ee-Peng Lim, Lidong Bing, Xing Xu, Soujanya Poria, and Roy Ka-Wei Lee. 2023. LLM-Adapters: An adapter family for parameter-efficient fine-tuning of large language models. In *Proceedings of the 2023 Conference on Empirical Methods in Natural Language Processing*.
- Sanjoy Dasgupta, Charles F Stevens, and Saket Navlakha. 2017. A neural algorithm for a fundamental computing problem. *Science*, 358(6364):793–796.

A Extended Related Work

From single-domain to learned-domain adaptation. The PEFT literature can be read as a search for the right *coordinate system* in which a small update is expressive. LoRA fixes the canonical (spatial) coordinates and constrains the update to be low

rank (Hu et al., 2022); AdaLoRA reallocates rank across layers (Zhang et al., 2023); DoRA decomposes magnitude and direction (Liu et al., 2024); VeRA freezes random projections and learns only scalings (Kopiczko et al., 2024); and orthogonal or Householder reparameterizations rotate the update within the spatial domain. Spectral methods change the coordinate system outright: FourierFT learns coefficients in the DFT basis (Gao et al., 2024), WaveFT in a wavelet basis (Bilican et al., 2025), and FouRA performs the low-rank projection itself in the Fourier domain, reporting that the resulting bases are decorrelated and merge well (Borse et al., 2024). CrossSpectra exploits the empirical observation that cross-layer adaptation energy is spectrally smooth (Zhang et al., 2025). FRAME unifies these views: rather than choosing the spatial or a fixed spectral coordinate system, it parameterizes the family of coordinate systems by the fractional order and learns where to sit, per expert and per token.

Mixture-of-experts adapters. MoE has a long history as a capacity-scaling mechanism (Jacobs et al., 1991; Shazeer et al., 2017; Lepikhin et al., 2020; Fedus et al., 2022; Dai et al., 2024), and its adapter incarnations include LoRAMoE (Dou et al., 2023), MixLoRA (Li et al., 2024), MoLE (Wu et al., 2024), MoLA (Gao et al., 2024), HydraLoRA (Tian et al., 2024), HMoRA (Liao et al., 2025), and extremely parameter-efficient soft-merging variants (Zadouri et al., 2024). Recent work questions the assumption that experts should be *homogeneous*: MoA mixes structurally different adapter types (Cao et al., 2026), and LD-MoLE makes the number of active experts token- and layer-dependent through differentiable routing (Zhuang et al., 2026). FRAME is in this heterogeneous-expert lineage, with domain (fractional order) as the axis of heterogeneity, and complements router-free designs that decorrelate experts through a frozen sparse random projection (Zou et al., 2025a) by making the decorrelating transform learnable rather than fixed.

Why fractional Fourier. The fractional-Fourier transform is standard in signal processing for analyzing chirped and non-stationary signals, precisely because it interpolates between time and frequency representations (Namias, 1980; Almeida, 1994; Ozaktas et al., 1996; Candan et al., 2000). Its relevance to learning is suggested by spectral-bias theory: neural networks learn low-frequency struc-

ture first (Rahaman et al., 2019; Xu et al., 2020), so different tasks and layers, which require different frequency content, should prefer different points between the time and frequency domains. To our knowledge FRAME is the first to use the fractional order as a learnable adaptation domain.

B Proofs

Throughout, Φ_a is the DFrFT of order a with spectral decomposition (2), $\theta = \frac{\pi}{2}a$, and $\mathbf{R}_a = \text{Re}\{\Phi_a\}$.

B.1 Proposition 1 (Strict generalization)

At $a=0$ we have $\theta=0$, so $\Phi_0 = \sum_m \mathbf{u}_m \mathbf{u}_m^\top = \mathbf{I}$ because $\{\mathbf{u}_m\}$ is an orthonormal basis; hence $\mathbf{R}_0 = \mathbf{I}$ and the expert update (3) is $\Delta W_i = B_i A_i$, identical to a LoRA expert. At $a=1$, $\theta=\frac{\pi}{2}$ and $\Phi_1 = \mathbf{F}$, the unitary DFT, so $\mathbf{R}_1 = \text{Re}\{\mathbf{F}\}$ is the real (cosine) part and the expert is a cosine-domain low-rank adapter of the FourierFT family with the same factor count. Thus both spatial and Fourier MoE-LoRA lie in FRAME’s hypothesis class. Strictness for $N \geq 2$: take two experts with $a_1=0, a_2=\frac{1}{2}$ and rank $r < d$. The realized update set $\{B_1 A_1 + B_2 A_2 \mathbf{R}_{1/2}\}$ contains matrices of rank up to $2r$ whose right singular vectors mix the canonical basis and the $\mathbf{R}_{1/2}$ -rotated basis; no single-order rank- r (or rank- $2r$ single-domain) family contains all such matrices because $\mathbf{R}_{1/2}$ is not a permutation of the identity eigenbasis. \square

B.2 Proposition 2 (Bounded order gradients)

Differentiating (2) in a and using $\theta = \frac{\pi}{2}a$,

$$\frac{\partial \Phi_a}{\partial a} = -i \frac{\pi}{2} \sum_m m e^{-im\theta} \mathbf{u}_m \mathbf{u}_m^\top. \quad (9)$$

This is a normal operator with eigenvalues $\{-i \frac{\pi}{2} m e^{-im\theta}\}$, so its spectral norm is $\frac{\pi}{2} \max_m |m|$. Restricting to the rank- ρ subspace $\text{span}\{\mathbf{u}_m\}_{m < \rho}$ gives $\|\partial \Phi_a / \partial a\|_2 \leq \frac{\pi}{2}(\rho - 1)$. Taking the real part is 1-Lipschitz, so the same bound holds for \mathbf{R}_a . For the per-token loss \mathcal{L} with $y = \dots + \frac{\alpha}{r} g_i B_i A_i \mathbf{R}_{a_i} x$,

$$\begin{aligned} \left| \frac{\partial \mathcal{L}}{\partial a_i} \right| &= \left| \langle \nabla_y \mathcal{L}, \frac{\alpha}{r} g_i B_i A_i \frac{\partial \mathbf{R}_{a_i}}{\partial a_i} x \rangle \right| \\ &\leq \frac{\alpha}{r} |g_i| \|\nabla_y \mathcal{L}\|_2 \|B_i\|_2 \|A_i\|_2 \frac{\pi}{2} (\rho - 1) \|x\|_2, \end{aligned} \quad (10)$$

by Cauchy–Schwarz and submultiplicativity, with $|g_i| \leq 1$. Hence the gradient is bounded and training is stable under a step size $\eta_a \leq 1/L_a$ with L_a the above bound. \square

B.3 Proposition 3 (Domain-diversity decorrelation)

Let $\Delta W_i = B_i A_i \mathbf{R}_{a_i}$ with independent factors, $\mathbb{E}[A_i^\top A_i] = \frac{1}{d} \mathbf{I}$, and likewise for B_i normalized so $\mathbb{E}\|\Delta W_i\|_{\text{F}}^2 = 1$. Using index additivity, $\mathbf{R}_{a_i} \mathbf{R}_{a_j}^\top = \text{Re}\{\Phi_{a_i}\} \text{Re}\{\Phi_{a_j}\}^\top$, and expanding the real parts,

$$\mathbf{R}_{a_i} \mathbf{R}_{a_j}^\top = \frac{1}{2} \text{Re}\{\Phi_{a_i - a_j}\} + \frac{1}{2} \text{Re}\{\Phi_{a_i + a_j}\}^\dagger, \quad (11)$$

where the first term depends only on the order *difference* and the second is an oscillatory chirp term that averages out. Taking expectations over the independent factors,

$$\mathbb{E}\langle \Delta W_i, \Delta W_j \rangle_{\text{F}} = \mathbb{E} \text{tr}(\mathbf{R}_{a_j} A_j^\top B_j^\top B_i A_i \mathbf{R}_{a_i}^\top) \quad (12)$$

$$= \frac{1}{d} \text{tr}(\mathbf{R}_{a_i} \mathbf{R}_{a_j}^\top) \mathbb{E} \text{tr}(B_j^\top B_i) c_r, \quad (13)$$

and the dominant term is proportional to $\text{tr} \text{Re}\{\Phi_{a_i - a_j}\}$. Normalizing and applying Cauchy–Schwarz over the r shared directions gives

$$\mathbb{E} \left[\frac{\langle \Delta W_i, \Delta W_j \rangle_{\text{F}}}{\|\Delta W_i\|_{\text{F}} \|\Delta W_j\|_{\text{F}}} \right]^2 \leq \frac{1}{r} \underbrace{\frac{1}{d} \|\text{Re}\{\Phi_{a_i - a_j}\}\|_{\text{F}}^2}_{\kappa(|a_i - a_j|)}. \quad (14)$$

Finally $\kappa(0) = \frac{1}{d} \|\mathbf{I}\|_{\text{F}}^2 = 1$, and for $\delta \in (0, 1]$ the energy of $\text{Re}\{\Phi_\delta\}$ spreads off the diagonal as δ grows (the eigenphases $e^{-im\theta}$ dephase), so κ is decreasing on $[0, 1]$ with $\kappa(1) = \frac{1}{d} \|\text{Re}\{\mathbf{F}\}\|_{\text{F}}^2$. \square

B.4 Proposition 4 (Faithful surrogate and complexity)

The Ozaktas decomposition writes the continuous FrFT as a chirp multiplication, a Fourier transform, and a second chirp multiplication; sampling at the Nyquist rate of the chirp-modulated signal yields (6) with discretization error $\mathcal{O}(d^{-1})$ in the band-limited regime (Ozaktas et al., 1996). The cost is two $\mathcal{O}(d)$ Hadamard products and one $\mathcal{O}(d \log d)$ FFT, hence $\mathcal{O}(d \log d)$ time and $\mathcal{O}(d)$ memory, against $\mathcal{O}(d^2)$ for the dense matrix in (2). The parameter accounting follows by counting active factors: k experts each contributing $r(d + d_{\text{out}})$, k order scalars, and the Nd router. \square

C Experimental Details

Data and evaluation. For commonsense reasoning we fine-tune on the merged training split

| Hyperparameter | Value |
|---|------------------------------|
| Experts N | 8 |
| Active experts k | 2 |
| Rank r per expert | 8 |
| Order bands G | 4 |
| Order init | uniform grid on $[0, 1]$ |
| Scaling α | 16 |
| Target modules | q,k,v,o,gate,up,down |
| Optimizer (matrices) | AdamW, lr 2×10^{-4} |
| Optimizer (orders) | AdamW, lr 2×10^{-5} |
| Balancing weight λ_{bal} | 10^{-2} |
| Epochs | 3 |
| Batch size (effective) | 128 |
| Precision | bfloat16 |
| Seeds | 3 |

Table 4: Default FRAME hyperparameters.

following the LLM-Adapters protocol and report test accuracy per dataset (Hu et al., 2023). For mathematical reasoning we train on the combined GSM8K/MATH/SVAMP/MAWPS/AQuA training questions and report exact-match accuracy; MATH is evaluated on the held-out test subset. For code we report pass@1 on HumanEval and MBPP with greedy decoding. For knowledge we report accuracy on MMLU (zero-shot) and ScienceQA. All evaluations use the same prompts across methods.

Hyperparameters. Table 4 lists the configuration. We tune only the FRAME-specific quantities (N , k , G , η_a) lightly on a held-out commonsense split and keep them fixed across task families and backbones; baselines use their recommended settings at matched rank. We use AdamW, cosine decay, 3 epochs, sequence length 512 (math/code/knowledge) or 256 (commonsense), and bfloat16.

Hardware. Experiments run on $8 \times$ NVIDIA A100 80GB GPUs. A commonsense run for an 8B backbone takes roughly 5 GPU-hours; the math/code/knowledge mixture takes roughly 9 GPU-hours. The chirp-FFT surrogate is implemented with the framework FFT and adds a single complex multiply on either side.

D Additional Results

Per-seed variation. Table 5 reports mean and standard deviation over three seeds for the commonsense average; FRAME’s improvements exceed one standard deviation for both backbones.

Additional backbones. Table 6 reports the commonsense average across backbone scales, support-

| Method | LLaMA-3.1-8B | Qwen2.5-7B |
|--------------|-----------------------------------|-----------------------------------|
| LoRA | 84.5 ± 0.20 | 85.9 ± 0.18 |
| FlyLoRA | 86.1 ± 0.17 | 87.3 ± 0.16 |
| FourierMoE | 86.2 ± 0.21 | 87.4 ± 0.19 |
| MoA | 86.3 ± 0.18 | 87.5 ± 0.17 |
| FRAME | 87.1 ± 0.15 | 88.2 ± 0.14 |

Table 5: Commonsense average over three seeds (mean \pm std).

ing Figure 5(c): the gain over the best baseline is stable from 1.5B to 14B.

| Method | 1.5B | 3B | 8B | 14B |
|--------------------|-------------|-------------|-------------|-------------|
| LoRA | 70.2 | 78.6 | 84.5 | 88.1 |
| Best baseline | 72.5 | 80.7 | 86.3 | 89.6 |
| FRAME | 73.6 | 81.7 | 87.1 | 90.4 |
| Δ over best | +1.1 | +1.0 | +0.8 | +0.8 |

Table 6: Commonsense average across model scales (Qwen2.5 family for 1.5B/3B/14B, LLaMA-3.1-8B for 8B). “Best baseline” is the strongest non-FRAME method at each scale.

Number of experts and active k . Table 7 sweeps N and k . Accuracy rises with N and saturates around $N=8$; $k=2$ is the best accuracy/cost point, with $k=1$ underfitting and $k=4$ adding cost without commensurate gain.

| Setting | Avg. | Param % | Rel. time |
|-------------|-------------|---------|-----------|
| $N=4, k=2$ | 86.6 | 0.21 | 0.95 |
| $N=8, k=1$ | 86.4 | 0.21 | 0.92 |
| $N=8, k=2$ | 87.1 | 0.31 | 1.00 |
| $N=8, k=4$ | 87.2 | 0.52 | 1.18 |
| $N=16, k=2$ | 87.2 | 0.34 | 1.06 |

Table 7: Effect of expert count N and active experts k on LLaMA-3.1-8B commonsense. Relative time is normalized to the default.

Method properties. Table 8 situates FRAME among representative baselines along the axes that matter for our claims.

E Training-Free Merging

To test whether domain diversity aids composition, we train single-task FRAME adapters independently and merge them by averaging their updates, then evaluate post-merge retention (the fraction of single-task accuracy preserved). Table 9 shows FRAME retains the most among the compared baselines. This matches Proposition 3: experts placed at diverse orders interfere less, so their sum is closer to the concatenation of the individual updates.

| Method | Domain | MoE | Routing | Learn. basis |
|--------------|-------------------|----------|---------|--------------|
| LoRA | spatial | × | × | × |
| FourierFT | Fourier | × | × | × |
| MixLoRA | spatial | ✓ | token | × |
| HMoRA | spatial | ✓ | token | × |
| FlyLoRA | spatial | implicit | random | × |
| FourierMoE | Fourier | ✓ | token | × |
| FRAME | fractional | ✓ | token | order |

Table 8: FRAME is the only method whose adaptation *domain* is a learnable, per-expert quantity on the spatial-spectral continuum.

| Method | Avg. retention | Worst-task |
|--------------|----------------|-------------|
| LoRA (avg.) | 71.3 | 58.0 |
| MixLoRA | 78.6 | 67.4 |
| FlyLoRA | 86.9 | 80.2 |
| FRAME | 87.8 | 81.6 |

Table 9: Training-free merging of four single-task adapters on LLaMA-3.1-8B: post-merge retention (%). Higher is better.

F Discussion

Why a learned domain helps. Three forces combine. *Compaction*: tasks whose update energy concentrates at intermediate time–frequency tilt are represented more compactly at the matching order, so a fixed basis wastes rank (Figure 1). *Diversity*: a mixture spanning orders covers more of the update space than the same number of single-domain experts (Proposition 1). *Decorrelation*: orders that are far apart are incoherent (Proposition 3), so experts specialize without redundancy and compose better. The first is about a single expert; the second and third are about the mixture.

Relation to projection-based decorrelation. Sparse or random projections decorrelate updates by mapping them into a high-dimensional space and keeping only the strongest responses (Dasgupta et al., 2017; McDonnell et al., 2023; Zou et al., 2025a,b), while orthogonal-subspace methods impose decorrelation by construction (Chaudhry et al., 2020; Wang et al., 2023). FRAME obtains decorrelation through a structured, *learnable* transform instead: the order plays the role a fixed projection plays in those methods, but it is differentiable, interpretable, and invertible. An interesting hybrid, left to future work, would combine random projections *and* fractional orders.

Beyond adapters. Nothing in FRAME is specific to LoRA factors. The fractional order is a property of the *domain* and could equally parameterize

a full-rank update, a per-head attention reweighting, or a continual-learning module that places new tasks at fresh orders to minimize interference with old ones. The bounded-gradient and decorrelation results carry over unchanged, suggesting the fractional domain is a general tool for controlling interference in adaptation.

Failure modes. When a task is genuinely well served by a single domain (e.g. a purely spatial edit), FRAME should and does collapse most experts to that order; the cost is then the unused order scalars and the FFTs, which is small but non-zero. When routing collapses, grouped balancing reactivates idle bands, but an adversarial data mixture could still starve a band; monitoring per-band utilization (Figure 4c) is a cheap diagnostic.